Higher order terms may be also obtained in the same manner. It is clear that (11) gives the regular two boundary conditions for the incident Rayleigh wave, whereas (12) gives the needed boundary conditions for solving the first-order scattered fields ϕ_1 and ψ_1. We may rearrange (12) into the following convenient forms:

$$\begin{aligned} L_1(\phi_1, \psi_1) &= 2\mu\lambda \frac{df}{dx} \left(\frac{\partial^2}{\partial x^2} \phi_i - \frac{\partial^2}{\partial z^2} \phi_i - 2 \frac{\partial^2}{\partial x \partial z} \psi_i \right) \\ &\quad - \mu\lambda f(x) \left(2 \frac{\partial^3}{\partial x \partial z^2} \phi_i - \frac{\partial^3}{\partial z^3} \psi_i + \frac{\partial^3}{\partial x^2 \partial z} \psi_i \right) \\ &= -P_1(x), \qquad \text{at } z = 0 \\ L_2(\phi_1, \psi_1) &= -\lambda_e \lambda f(x) \left(\frac{\partial^3}{\partial x^2 \partial z} \phi_i + \frac{\partial^3}{\partial z^3} \phi_i \right) \\ &\quad - 2\mu\lambda f(x) \left(\frac{\partial^3}{\partial z^3} \phi_i + \frac{\partial^3}{\partial x \partial z^2} \psi_i \right) \\ &= -Q_1(x), \qquad \text{at } z = 0. \end{aligned} \tag{13}$$

It is seen that (13) represents stresses T_{zx} and T_{zz}, respectively, on the unperturbed surface $z=0$. These nonzero stresses are due to the interaction between the incident Rayleigh wave and the guiding surface deformation. Hence, (13) may be considered as a sheet of first-order line sources which generate the first-order scattered fields ϕ_1 and ψ_1. Similarly, we may obtain mth-order sources which will be in terms of the incident Rayleigh wave and lower order scattered fields up to $(m-1)$. The perturbation method used here is clearly a replacement of the original boundary condition on S by some induced distribution of sources on the unperturbed surface at $z=0$.

With the help of (5) and (6), the solution for ϕ_1 and ψ_1 may be written as

$$\phi_1(x, z) = \frac{-1}{2\pi\mu} \int_{-b}^{b} \int_{-\infty}^{\infty} \frac{+2k\xi_2 P_1(x') + (2k^2 - k_2{}^2) Q_1(x')}{F(k)} \cdot e^{ik(x-x')} e^{-i\xi_1 z} \, dk dx' \tag{14}$$

$$\psi_1(x, z) = \frac{1}{2\pi\mu} \int_{-b}^{b} \int_{-\infty}^{\infty} \frac{(2k^2 - k_2{}^2) P_1(x') - 2k\xi_1 Q_1(x')}{F(k)} \cdot e^{ik(x-x')} e^{-i\xi_2 z} \, dk dx' \tag{15}$$

where $P_1(x')$ and $Q_1(x')$ are given by (13) replacing x by x', and $-b$ to b is the range for which $f(x)$ exists. The path of integration is along the real axis of the complex k plane shown in Fig. 2. It is seen that the first-order scattered fields depend on the shape of the surface deformation through the dependence of variable x'. The second-order scattered fields are found as follows. Firstly, obtain the equivalent line source distribution $P_2(x')$ and $Q_2(x')$ from the third-pair coefficient functions of ϵ^2 in the Taylor series expansion. Then, $\phi_2(x, z)$ and $\psi_2(x, z)$ may be obtained with the repeated help of the Green's functions (5) and (6). Similarly, all other higher order scattered fields proposed in (8) may be found in the same manner.

V. Discussion and Conclusion

The evaluation of (14) and (15) may be carried out with the help of the contour integration technique. It can be shown that the reflected surface wave is due to the pole contribution at $k=-k_r$. The expression may be obtained quite easily. The bulk wave radiated into the substrate is contributed by two branch cut integrations along C_1 and C_2, shown in Fig. 2. The leading term for the far field may be obtained by the steepest descent integration technique. The details of these are omitted here, as similar calculations are given in (11). To design the discontinuity for purpose of tapping Rayleigh waves, we need to properly select the function $f(x)$ and the value of ϵ. As the bulk-wave power coupled out at the tap is proportional to ϵ^2, the direction of propagation depends on the exact geometric shape of the surface deformation. In an actual device, only a small portion of the incident power is used at each tap. Naturally, it requires a deformed surface contour with small ϵ value. Therefore, the perturbation formulation of this type of discontinuity is believed to give an approximate solution.

References

[1] *IEEE Trans. Microwave Theory Tech.* (*Special Issue on Microwave Acoustics*), vol. MTT-17, Nov. 1969.

[2] *Microwave J.* (*Special Issue on Microwave Acoustics*), vol. 13, Mar. 1970.

[3] J. H. Collins and P. J. Hagon, "Surface wave delay lines promise filters for radar, flat tubes for television and fasten computers," *Electronics*, vol. 43, Jan. 1970.

[4] E. Stern, "Microwave components, circuits and applications," Lincoln Lab. Tech. Note 1968-36, Oct. 1968.

[5] L. R. Adkins, T. W. Bristol, P. J. Hagon, and A. J. Hughes, "Surface acoustic waves—Device applications and signal routing techniques for VHF and UHF," *Microwave J.*, vol. 13, Mar. 1970.

[6] W. R. Smith *et al.*, "Analysis of interdigital surface wave transducers by use of an equivalent circuit model," *IEEE Trans. Microwave Theory Tech.* (*Special Issue on Microwave Acoustics*), vol. MTT-17, pp. 856–864, Nov. 1969.

[7] ——, "Design of surface wave delay lines with interdigital transducers," *IEEE Trans. Microwave Theory Tech.* (*Special Issue on Microwave Acoustics*), vol. MTT-17, pp. 865–873, Nov. 1969.

[8] A. P. Van Den Heurel, D. B. Owen, and S. G. Joshi, "Hybrid transducer: A new technique for generating surface waves on non-piezoelectric substrates," presented at the IEEE G-SU Ultrasonics Symp., St. Louis, Mo., Sept. 1969, Paper C-8.

[9] W. C. Wang, P. Staecker, and R. C. M. Li, "Elastic waves bound to a fluid layer between two adjacent solids," *Appl. Phys. Lett.*, vol. 16, Apr. 1970.

[10] R. C. M. Li and K. H. Yen, "Elastic waves guided by a solid layer between adjacent substrates," *IEEE Trans. Microwave Theory Tech.*, vol. MTT-20, pp. 477–486, July 1972.

[11] H. S. Tuan and C. P. Chang, "Tapping of Love waves in an isotropic surface waveguide by surface-to-bulk wave transduction," *IEEE Trans. Microwave Theory Tech.*, vol. MTT-20, pp. 472–477, July 1972.

[12] P. M. Morse and H. Feshback, *Methods of Theoretical Physics*, vol. 2. New York: McGraw-Hill, 1953, ch. 9.

[13] Y. M. Chen and S. J. Kim, "Scattering of acoustic waves by a penetrable sphere with statistically corrugated surface," *J. Acoust. Soc. Amer.*, vol. 42, July 1967.

[14] R. E. Collin, *Field Theory of Guided Waves.* New York: McGraw-Hill, 1960, ch. 11.

[15] I. Abubakar, "Scattering of plane elastic waves at rough surfaces I, II," *Proc. Cambridge Phil. Soc.*, vol. 58 and 59, 1962.

[16] B. A. Auld, "Application of microwave concepts to the theory of acoustic fields and waves in solids," *IEEE Trans. Microwave Theory Tech.* (*Special Issue on Microwave Acoustics*), vol. MTT-17, pp. 800–811, Nov. 1969.

Coupling Errors in Cavity-Resonance Measurements on MIC Dielectrics

P. H. LADBROOKE, M. H. N. POTOK, AND E. H. ENGLAND

***Abstract*—Measurements on MIC dielectrics have been made by applying the theory of resonant cavities to either wholly or partly metallized substrates. Two different schemes of coupling are employed, depending upon the metallization. Errors occur in the derived value of ϵ, due to the coupling, and are of opposite sense for the two methods discussed. They may be averaged to improve the overall measurement precision (0.5 percent).**

Several authors have recently described a convenient way of measuring the permittivity of MIC substrate materials [1], [2], [6]. The substrate, which may typically be 2.5 cm square by 0.5 mm thick for Al_2O_3 (alumina and sapphire) and 1.5–2 times larger for quartz, is simply metallized on some or all of its faces, and cavity resonances are excited in it from which ϵ may be deduced. We have used both completely and partly metallized cavities to measure ϵ for 15 samples of Al_2O_3 and find a scatter of a few percent in the experimental data which is related to the perturbation of the cavity fields at the coupling points, the coupling method being different for the two different metallization schemes. These two methods lead to errors of opposite sense, and hence yield a more accurate averaged value for ϵ than if either set were used alone. Of more immediate interest to the practicing engineer is the finding that certain specific resonances require no correction at all, yielding quick and accurate answers.

The basic structures investigated are shown in Fig. 1. In Fig. 1(a), the two large faces are metallized, but the sidewalls are left uncoated [1]. Excitation and detection are effected at the corners using the HP 8410A/8740A network analyzer system [1]. We refer to such cavities as having open-circuit or magnetic sidewalls. For Fig. 1(b), the substrate is metallized all over, and two apertures are photolithographically cut: one for excitation via an overlaid stripline 3 mm in diameter at $(y_1/5, z_1/5)$ in the broad face and the other (smaller) 1 mm long in a sidewall for detection via a loop probe. This device we refer to as having short-circuit or electric sidewalls.

In trying to establish a philosophy for coupling with coated edges, we first of all tried cutting two apertures in the sidewalls; however, with this arrangement, only a few of the modes possible could be found—mainly due to there being no probe penetration into the solid dielectric. A broadwall hole with overlaid stripline provides tighter

Manuscript received November 30, 1972, revised February 15, 1973.
The authors are with the Department of Electrical and Electronic Engineering, Royal Military College of Science, Shrivenham, Swindon, Wilts., England.

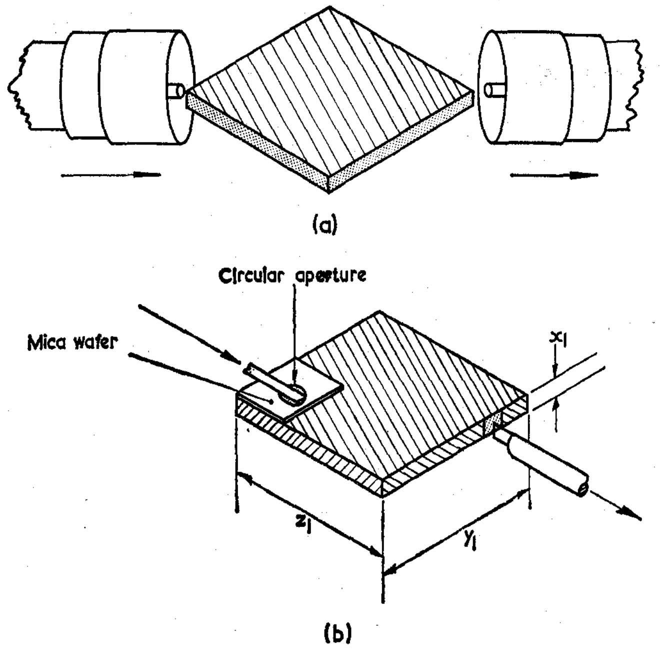

Fig. 1. Resonator configurations. (a) Magnetic (uncoated) sidewalls. (b) Electric (coated) sidewalls.

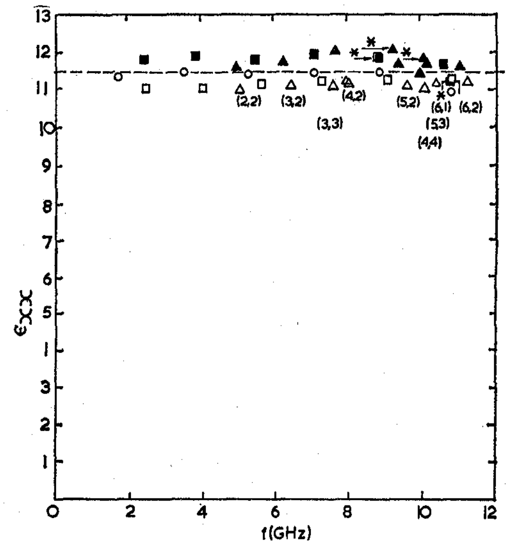

Fig. 2. Typical experimental result for ϵ_{xx} (example for c-axis sapphire). Points marked * illustrate the effect of reduced coupling.

coupling for a given aperture size, and the energy transfer into and out of the cavity is adequate without having to make the apertures unacceptably large. We tried to capitalize on this property by using one broadwall hole and one sidewall aperture, with the latter reduced to the point of contributing negligibly to the overall perturbation.

It may be proved by textbook methods [3] that the waves excited in both cavity types are TE only. (Note that when ϵ is a tensor, as with sapphire, the principal axes of the crystal must be aligned with the resonator coordinates for this to remain true.) For both magnetic and electric sidewalls, the relative dielectric constant along the thin (x) direction is then related to the eigenfrequencies by

$$\epsilon_{xx} = \frac{c^2}{f_{n,m}^2}\left\{\left(\frac{n}{2y_1}\right)^2 + \left(\frac{m}{2z_1}\right)^2\right\}. \tag{1}$$

[A mode chart based upon (1) has been found helpful for preliminary identification of the detected resonances; such a chart requires plotting log (ϵ_{xx}) versus log (f) for $y_1 = z_1 = 2.5$ cm, say, and may be used for a square substrate of any side by scaling ϵ_{xx} inversely as the dimension squared, cf. (1).]

An example of ϵ_{xx} computed in the range 2–12 GHz for the c axis of sapphire illustrates the aforementioned scatter in points (Fig. 2). The dotted line represents the arithmetic mean of the modes common to both test configurations, that is, the (1, 1) and higher order resonances. Without exception, for all 15 samples the data were distributed in the same manner.

It is our contention that the above phenomenon is governed by the reactive effects of perturbing the cavity fields at the coupling points. These effects may be estimated by the well-known perturbation theory, which relates frequency shifts to changes in electric and magnetic energies stored within the cavity. In normalized terms [4], [5],

$$\frac{\omega^2 - \omega_0^2}{\omega_0^2} \sim \int_{\Delta\tau} (E^2 - H^2)\, dv \tag{2}$$

where ω_0 is the undisturbed frequency and $\Delta\tau$ represents an increment in the volume occupied by the fields.

At magnetic sidewalls, $\boldsymbol{n}\times\boldsymbol{H} = 0$; the lines of the $\boldsymbol{H}$ field close in the space exterior to the cavity itself and, with the exception of the (n, 0) modes, form loops at the resonator corners of the same configuration as H_ϕ in the coaxial feedline. At the coupling point, however, $\boldsymbol{E}$ is caused to fringe into an effective volume $\Delta\tau$ determined by the conductor sizes of the line. The perturbation is therefore principally to the electric field just inside the corner of the resonator [Fig. 3(a)]. It must be stressed that the zero-order resonances are a special case in that H_y (or H_z) is everywhere zero (i.e., $\boldsymbol{n}\cdot\boldsymbol{H} = 0$ along

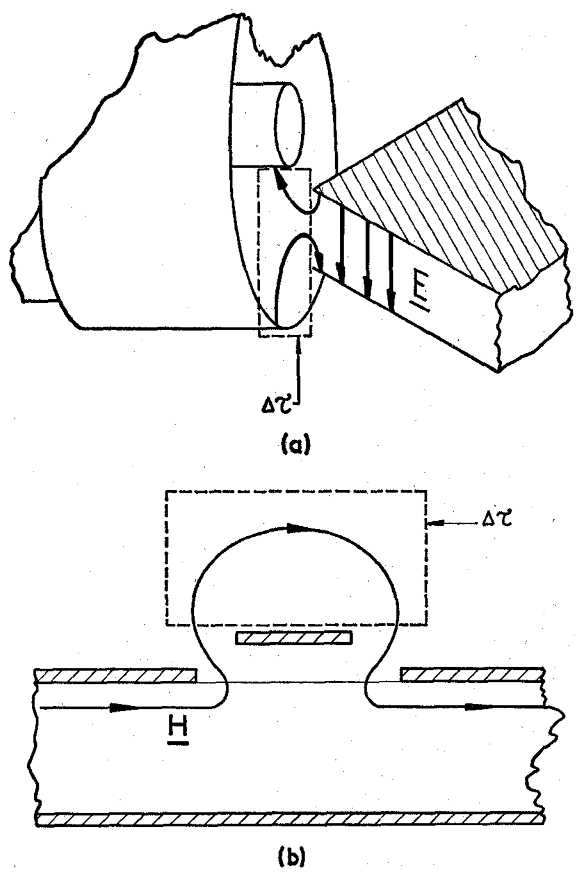

Fig. 3. Field perturbation at coupling points. (a) Corner coupling. (b) Aperture coupling.

two edges), so the magnetic fields of the resonator and coax are not compatible over the coupling volume. Inasmuch as field from the coax will penetrate into these two edges where $\boldsymbol{H}$ is normally zero, an increase in the magnetic stored energy is to be expected, implying a nonnegligible contribution from the magnetic term in (2) and at least a partial cancellation of the frequency error—a fact we shall demonstrate by ignoring this contribution when calculating the

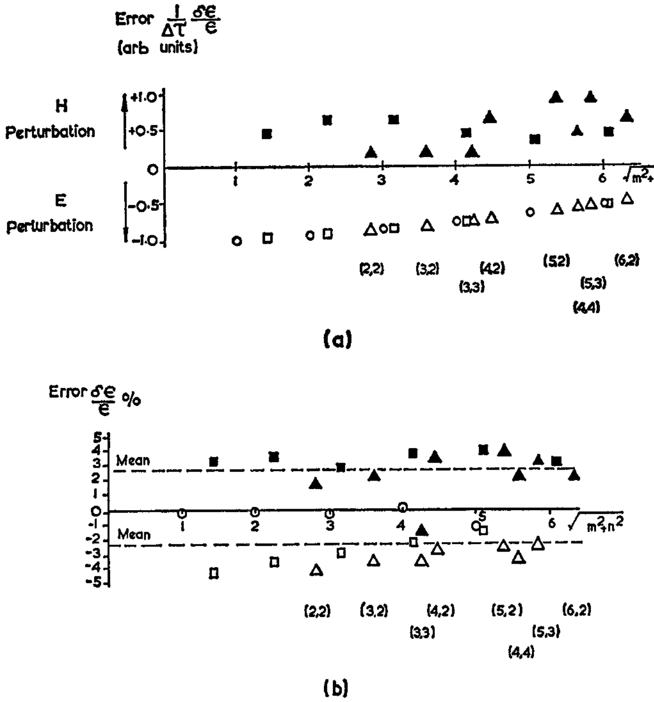

Fig. 4. Mode errors in ϵ_{xx}. (a) Theoretical. (b) Experimental (averaged over 15 samples).

theoretical error and seeing if, as a consequence, there results a discrepancy between theory and experiment that can be accounted for qualitatively by the omitted (magnetic) term (see the discussion on Fig. 4).

For electric sidewalls, $\boldsymbol{n}\cdot\boldsymbol{H}=0$ at all interior metal surfaces. The cutting of an aperture replaces an element δS of this surface by $\delta S'$, at which $\boldsymbol{n}\times\boldsymbol{H}=0$, and across which the magnetic field must pass normally [Fig. 3(b)]. Insofar as the overlaid stripline constitutes an unchanged boundary condition for $\boldsymbol{E}$, there is a comparatively small change in the electric field, so that the second term in (2) dominates the frequency shift for this coupling method. The effect upon ϵ_{xx} can be calculated from the following equation, derived from (1) and (2):

$$\frac{\delta\epsilon}{\epsilon_{xx}}\bigg|_{m,n} \alpha \int_{\Delta\tau} (H^2 - E^2)\, dv. \tag{3}$$

If the variation in phase over the coupling regions is neglected, and account is taken of only the electric contribution for the $(n, 0)$ frequencies, the error as a function of mode index $\sqrt{m^2+n^2}$ comes to the values set out in Fig. 4(a). The corresponding experimental points, expressed as averages over the 15 samples, are given in Fig. 4(b). Except for the $(n, 0)$ modes, the relative placement of the error points is broadly correct. The discrepancy for the zero-order resonances clearly shows that the magnetic energy in the cavity is increased by the field penetrating from the lines into the edges normally having $\boldsymbol{n}\cdot\boldsymbol{H}=0$, as was discussed in the application of (2) to the magnetic-sidewall cavity, and has the desirable effect of reducing the measurement error, in our experiments, to within 0.5 percent of the mean defined in Fig. 2. Hence, these modes alone may be used without correction for an accurate characterization of the dielectric over the band.

In general, the observed effect of decreased coupling is to reduce the error for magnetic sidewalls, but to increase it, if anything, for electric sidewalls (see Fig. 2). With corner excitation, the lower bound on the coupling is set by the sensitivity of the apparatus, and in the above experiments gave a mean error in ϵ_{xx} of -2.2 percent with all modes discernable [lower mean in Fig. 4(b)]. The result for aperture excitation can be understood if the feeding stripline is considered as a current boundary condition which limits the leakage of magnetic field $\boldsymbol{H}$. The mean error in this case was $+2.7$ percent [upper mean in Fig. 4(b)]. Thus for any given sample, the permittivity averaged over all modes (which neglects possible dispersion effects) should be within order 0.5 percent of the true value (Fig. 2 gives an example).

TABLE I

Material	Relative Permittivity ϵ_{xx}
Al_2O_3(96%)	8.76
Crystalline Al_2O_3 ("sapphire")	9.34 (base plane) 11.49 (c-axis)
SiO_2 (Fused quartz)	3.85

In conclusion, we have shown that, depending upon the equipment sensitivity, errors of 2–3 percent in the dielectric constant, as deduced from cavity-resonance measurements, can arise from the system of coupling. Two complementary methods of excitation have been described which, because they give rise to errors of opposite sense, improve the accuracy of the averaged dielectric constant to order 0.5 percent. For quick answers requiring no correction, the zero-order resonances of an uncoated sidewall cavity can be used to accurately measure the dielectric constant over the band. Our results for the common materials in the frequency range 2–12 GHz as determined by these methods are shown in Table I.

Acknowledgment

The authors wish to thank J. Tame and Mrs. C. Garrett for their assistance in metallizing the samples, and Dr. H. F. Lenzing of Bell Telephone Laboratories for a reprint of [2].

References

[1] L. S. Napoli and J. J. Hughes, "A simple technique for the accurate determination of the microwave dielectric constant for microwave integrated circuit substrates," *IEEE Trans. Microwave Theory Tech.* (Corresp.), vol. MTT-19, pp. 664–665, July 1971.
[2] H. F. Lenzing, "Measurement of dielectric constant and ceramic substrates at microwave frequencies," *Amer. Ceram. Soc. Bull.*, vol. 51, p. 361, 1972.
[3] R. E. Collin, *Field Theory of Guided Waves.* New York: McGraw-Hill, 1960.
[4] J. C. Slater, *Microwave Electronics.* Princeton, N. J.: Van Nostrand, 1950.
[5] E. L. Ginzton, *Microwave Measurements.* New York: McGraw-Hill, 1957.
[6] J. Q. Howell, "A quick accurate method to measure the dielectric constant of microwave integrated-circuit substrates," *IEEE Trans. Microwave Theory Tech.* (Short Paper), vol. MTT-21, pp. 142–143, Mar. 1973.

Equivalent Representation of an Abrupt Impedance Step in Microstrip Line

R. HORTON

***Abstract*—The equivalent electrical lengths of uniform microstrip line associated with an abrupt impedance step are first evaluated, under static assumptions. The importance of these results in establishing a reference plane for the step, and in the application of calculations of capacitance associated with the step, is then demonstrated.**

Furthermore, some interesting dualities are discerned from the results.

Introduction

The evaluation of equivalent circuits associated with common microstrip discontinuities has recently been a subject of intense interest in the microwave field, and the analysis of discontinuities causing predominantly capacitative effects, such as open-circuits or gaps, has received much attention from such workers as Farrar and Adams [1], Silvester and Benedek [2], Jain *et al.* [3], and Maeda [4].

However, discontinuities with associated inductive and capacitative effects, such as bends, impedance steps, and T junctions, have received less attention to date, due to the more involved problem. Nevertheless, attempts have been made by Wolff *et al.* [5], Horton

Manuscript received December 14, 1972; revised April 2, 1973.
The author is with the Advanced Techniques Branch, Australian Post Office, Research Laboratories, Melbourne, Vic., Australia.